

MEMS Spring Orientation

Rayna Arora, Ali Cy, and Win Win Tjong

Abstract—Different MEMS springs were designed by varying the orientation of the springs on the wafer. These spring designs are then fabricated using a special method called deep reactive ion etching (DRIE), which left the device at the top layer and removed the handle layer beneath the springs. Then each of the distinct springs was tested with interference microscopy and a Bluetooth speaker. The Bluetooth speaker is used to perform a frequency sweep to find the resonant frequency of the spring. The frequency can be used in relation to the Young's modulus to find how the stiffness of the spring is affected due to orientation. The data collected from the test suggest that there is a connection between the orientation of the MEMS spring design and the mechanical property of the spring.

Index Terms—MEMS springs, resonant frequency, DRIE

I. INTRODUCTION

SINCE their commercialization over forty years ago, microelectromechanical systems (MEMS) have seen a wide variety of uses and comprise an industry worth over \$15 billion today [1]. Different MEMS devices operate based on different underlying physical mechanisms. One such mechanism is that of resonance frequency: within a narrow range of the resonance frequency, the device vibrates readily at the same frequency in response. Both the narrow range of response, as well as amplitude magnification effect that is achieved with a high quality factor, are utilized in applications such as radio-frequency filters, resonant microscanners, and vibrating structure gyroscopes. Such applications often have strict tolerances for deviations in the resonant frequency, as narrow as 1,000 ppm or less [2]. In practice, this is achieved through additional components or techniques that tune the resonant frequency in response to variations due to manufacturing or environmental conditions such as temperature.

We study the manufacture of MEMS devices in single-crystal silicon. Manufacturing processes with single-crystal silicon are already well-established, leading to its popularity in MEMS applications as well. However, owing to its crystal structure, single-crystal silicon behaves in an orientation-dependent manner. Orientation affects many physical, chemical, and electrical properties of single-crystal silicon, such as thermal expansion, etching rate, and dopant solubility. Because of this, as well as the need to determine resonance frequencies precisely and reliably, the dependence of device resonance frequency on orientation within single-crystal silicon needs to be characterized.

Using a simple spring design fabricated on a silicon-on-insulator (SoI) wafer, we characterize the dependence of resonance frequency on orientation and provide a theoretical explanation of our results. We experimentally demonstrate that the resonance frequency can vary significantly, by at least 10%, simply due to rotation of the device within the crystal plane. This effect is characterized with a varying number of spring

beams, including two, three, and four beams. We provide a theoretical explanation of this effect owing to the directional dependence of Young's modulus in single-crystal silicon [3]. Overall, we demonstrate a clear, theoretically-justified effect of orientation on the resonance frequency of a MEMS spring.

II. METHODS

A. Design

We intend to investigate how the resonance of a MEMS spring changes when we vary both the orientation of the design and the number of bars on the spring. We fabricated springs with 2, 3, and 4 beams. We chose 5 different orientations for the 4-beam springs, and 3 orientations each for the 2- and 3-beam springs. No other design parameters were varied.

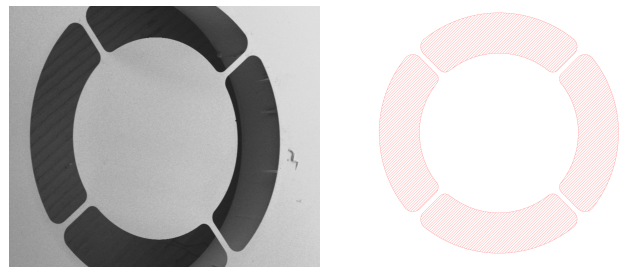


Fig. 1: Left: SEM image of this spring after fabrication, viewed at an angle, with some visible debris. Right: Corresponding spring design. Shown here is a 4-beam spring with 45° offset. The entire spring has a diameter of 2.25mm.

Springs with a beam pointing directly rightwards, a direction parallel to the crystal lattice, are said to have a 0° offset. Other springs can be determined to have a relative offset to the springs of 0° offset by how close the nearest beam is to the rightwards direction.

B. Fabrication

Our design had 25 springs, arranged in a 5×5 grid. We fabricated it on two silicon-on-insulator (SoI) wafers, which had top silicon layers of 9 and 23 μm , respectively. We used the design shown in Fig. 1. The bottom Si layers of the wafers are several hundred microns thick, about 30 times thicker than the device layer, providing a stable base for vibration.

To pattern each side, we used photolithography followed by deep reactive ion etching (DRIE) with sulfur hexafluoride (SF_6) as the etchant gas. We used AZ 10XT positive photoresist and exposed it with the MLA machine. We applied a $2\mu\text{m}$ thick layer of photoresist with the PicoTrack machine for the thin device side and manually applied a $10\mu\text{m}$ thick layer for the thick bottom side. Before DRIE on the back side, we mounted the device side onto a quartz wafer using SantoVac grease to protect the devices.

We stopped the DRIE process when the etched areas were no longer shiny, indicating removal of the silicon layer. We then used reflected light microscopy to ensure the distance between the top of the wafer to the etched regions was indeed the full width of the top wafer. Then, we stripped off the remaining photoresist with the ash, and again used reflected light microscopy to measure the depth etched.

To remove the SantoVac grease, we soaked the wafer in acetone for 3 days. We then separated the quartz from the silicon wafer. We rinsed the SOI wafer in a static water bath and air-dried it to prevent agitation. We did a final 15-minute etch with BOE to remove the oxide. We again rinsed it in a static water bath and air-dried it before testing.

Our design initially lacked alignment marks, so we used the top tangent points of two designated springs in the middle column for alignment. This does not seem to have affected the devices.

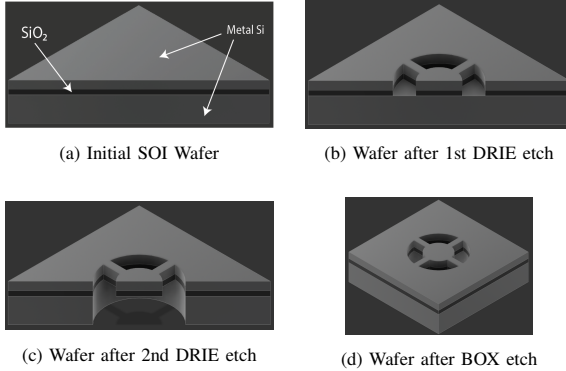


Fig. 2: Wafer diagrams along the fabrication process

C. DRIE: Deep Reactive Ion Etching

We used DRIE to achieve a high aspect ratio etch. We used the DRIE-STS-MMplex machine and the Bosch process. The SOI wafer with a mask of photoresist is put into the machine. First, the machine applies the passivation gas of C_4F_8 as a teflon coating. Then, SF_6 , the etch gas, is used and fluorine ions selectively etch downward, as shown. This process is repeated iteratively to achieve a high aspect ratio. During the process, helium cools the wafer from the bottom, preventing overheating. Etching stops once the middle oxide layer is reached.

D. Testing

Our test setup is shown in Fig. 3. We placed the wafer on top of two supports and placed the speaker in between them. We calibrated the reflected light microscope so that the interference pattern appeared on the center of the spring. We then performed a frequency sweep between 10 and 20,000 Hz, stopping when the interference pattern disappeared on the spring but not the surrounding wafer, indicating resonance (see Fig. 4).

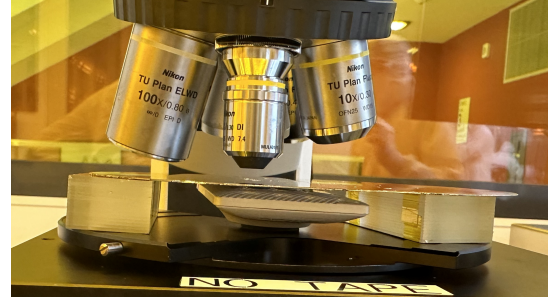


Fig. 3: Test setup to assess resonance.

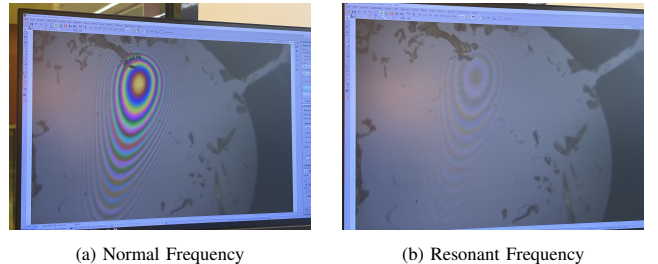


Fig. 4: Reflected light microscopy patterns on a spring while most frequencies are playing versus its resonant frequency.

III. RESULTS AND DISCUSSION

A. Qualitative Assessment of Device

We manufactured devices on two wafers, one with a device layer thickness of $9\mu m$ and another with a device layer thickness of $23\mu m$. We discarded the $9\mu m$ wafer in our analysis as many springs were no longer intact after fabrication. On the $23\mu m$ wafer, many of the suspension beams of the springs did not lay flat. They bowed either upward or downward, causing the spring's mass to sag. We measured the vertical displacement from the center of the spring to the wafer with reflected light microscopy. We found that the sagging effect varied amongst the devices, with a range of $4\mu m$ to $19\mu m$. Sagging was a bit more extreme for two-beam springs, which may explain their deviation from theoretical predictions. We also observed that in some places, the oxide was not completely etched. As the leftover pieces were not in contact with the device, we do not expect them to affect our results.

We additionally found that the springs typically responded to a range of resonance frequencies. The size of the range varied from approximately 30 Hz to 450 Hz. We did not find any obvious correlation between the size of the range and any design parameters. We used the midrange ($\frac{\min+\max}{2}$) as the resonance frequency. Some springs with two beams also had two resonance frequency bands; it is unclear to us why. We used the lower midrange. Using the higher midrange instead would not have significantly changed our results.

B. Quantitative Assessment of Device

We first examine the overall fit between our theoretical predictions and our empirical findings, shown in Fig. 6. There is a good correlation between the theoretical and predicted values, with an R^2 of 0.86. However, while the predicted

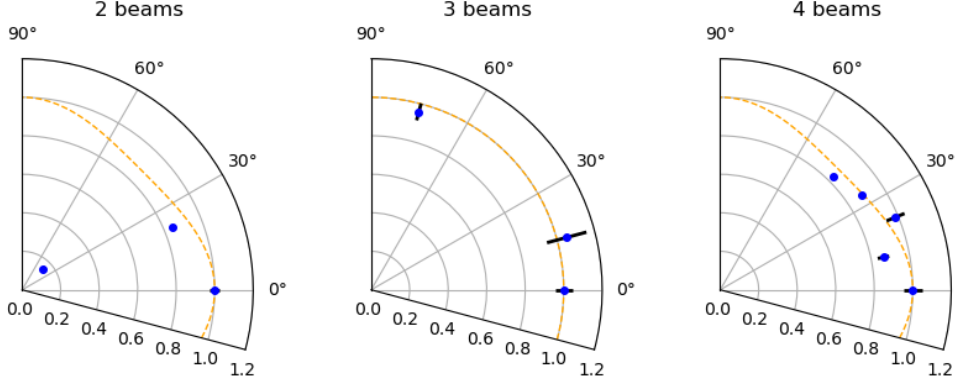


Fig. 5: Orientation dependence of resonance frequency f . Measured values f are represented as blue points with 95% confidence intervals, while the theoretical predictions of f are shown as dashed orange lines. 0° offsets are normalized to 1 (different normalization values are used for theoretical and predicted values), isolating the effect of orientation alone. Orientation dependence can clearly be observed and generally matches theoretical predictions.

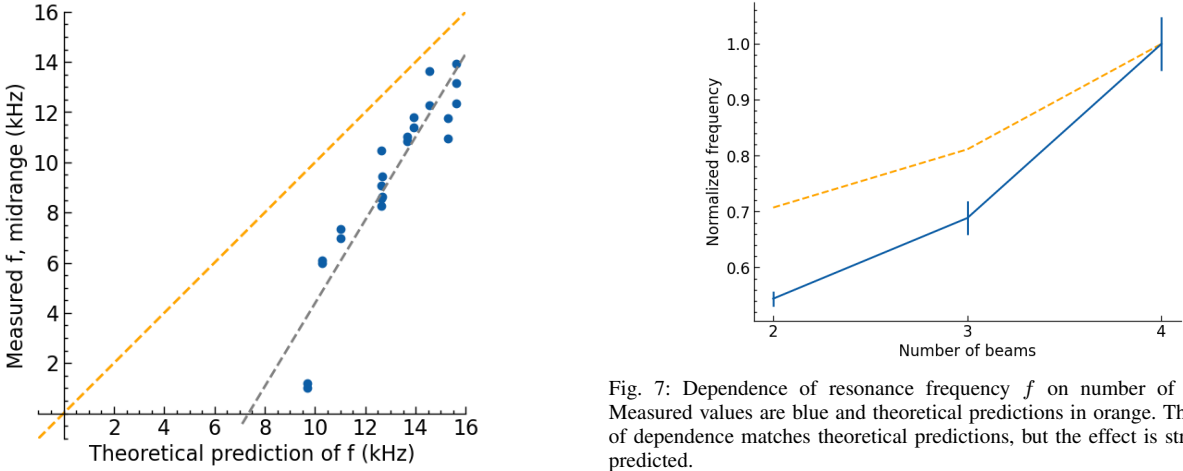


Fig. 6: Theoretical predictions of the resonance frequency f against the measured values. The line of best fit is $f_{\text{measured}} = 1.7f_{\text{theory}} - 12.2$ with an R^2 of 0.86, in gray. For comparison, the orange line is $f_{\text{measured}} = f_{\text{theory}}$, an exact match.

resonance frequency is rather accurate at high values, with a difference of around 20% from the measured frequency, it becomes non-predictive at low values, such as when there are only 2 beams. For example, for the 2 beams and 0° offset case, the predicted f is around 9.6 kHz while the actual f is around 1 kHz.

We next examine the orientation dependence for two, three and four beams (Fig 5). In order to isolate orientation dependence, we normalize the resonance frequencies at 0° offset to 1, for both theoretical and measured values. We can observe that in 2 and 4 beams, the lowest f are seen with a 45° offset, as predicted. With 4 beams, the reduction due to the 45° rotation is 17%, which closely matches the theoretical decrease of 13%. Additionally, with 3 beams, the effect of a 15° offset in either direction has minimal impact on the resonance frequency, as predicted.

There are some caveats to these conclusions. For one, the orientation dependence effect seems stronger at 11.25° offset than at 22.5° offset for 4 beams. Additionally, the effect is much stronger than anticipated for 2 beams, where the 45°

Fig. 7: Dependence of resonance frequency f on number of beams N . Measured values are blue and theoretical predictions in orange. The direction of dependence matches theoretical predictions, but the effect is stronger than predicted.

offset beam has a resonance frequency f of less than 20% of its 0° counterpart. This may be due to the fact that the 2 beam springs are more fragile, and perhaps its behavior is affected by additional orientation-dependent parameters beyond the Young's modulus.

Finally, we characterize the dependence of resonance frequency f on the number of beams N in Fig. 7. To minimize any effect from orientation, we only analyze zero-offset springs. Once more, we normalize the 4 beam spring to 1, to isolate the effect of beam number only. The predicted dependence of resonance frequency is roughly \sqrt{N} , but can be affected due to whether or not N aligns with the symmetry of the crystal lattice. We find that decreasing the number of beams decreases the resonance frequency as well, but the decrease is larger than predicted. While theoretically the 2-beam spring should only have f lower than 29% compared to the 4-beam spring, we instead observe a decrease of 46% in practice.

To summarize our results, we show a clear relationship between resonance frequency and two design parameters: the orientation of the spring, as well as the number of spring beams. The measured effects generally match the theoretical predictions made by the Young's modulus model presented in the following section, but not entirely. The theoretical model matches well for 4-beam springs and 3-beam springs (to a

lesser extent). Deviations are mostly due to two-beam springs having significantly lower Young's moduli than predicted, as well as some other anomalies. They may be due to the general fragility of the two-beam spring, the sagging effect, as well as orientation-dependent effects. The latter is suggested by how the two-beam spring with maximal offset deviated the most from the theoretical model.

In future work, we would like to vary more design parameters of the springs, including beam length, thickness, mass, or the overall size of the spring. We would also like to fabricate more devices and run more trials, as we could only fabricate two copies of most of the springs. Experimental design could be improved by adding alignment marks as well as using low-stress SoI wafers to prevent sagging. The two-beam springs need to be further examined in particular. We would also like to demonstrate this effect in a more complex system, such as one where the resonance frequency is used in downstream applications.

IV. THEORY

Suppose we use spring beams with length L , width w , and thickness $t \ll L$. A spring with one side fixed and with a single beam of the other side of the spring mass has a spring constant k of $\frac{Ewt^3}{L^3}$, which can be determined by calculating the displacement of the spring under a given force with Euler-Bernoulli beam theory [4], [5]. This derivation is valid as long as the beam is thin and long and the vertical displacement is relatively small. As the forces from each spring beam add up, a spring with multiple beams can be modeled as multiple springs—each with a single beam—placed in parallel. Thus, if E_i is the Young's modulus of the i th bar, the spring constant of the entire spring is

$$k = \frac{wt^3}{L^3} \cdot \sum_{i=1}^n E_i \quad (1)$$

The resonance frequency of a spring is well-known to be related to the spring constant via the equation $f = \frac{1}{2\pi} \sqrt{\frac{k}{m}}$. Given that all other design parameters of the spring are held constant, we thus get

$$f \propto \sqrt{\sum_{i=1}^n E_i} \quad (2)$$

Therefore, the resonance frequency depends on both the number of beams as well as the orientation of each beam within the crystal lattice.

Hopcroft et al. in [6] give a comprehensive characterization of the Young's modulus in silicon, including its orientation dependence. The Young's modulus varies between 130 GPa in the $\langle 100 \rangle$ direction and 188 GPa in the $\langle 111 \rangle$ direction. Within the (100) plane, however, the highest Young's modulus is 169 GPa, achieved in the $\langle 110 \rangle$ or $\langle \bar{1}10 \rangle$ directions, which are perpendicular to each other. The equation (9) in [6], which yields the Young's modulus E_α along a direction with offset α can be simplified for our purposes to:

$$E_\alpha = \left(a - b \cdot \frac{1 + \cos 4\alpha}{4} \right)^{-1}, \quad (3)$$

where $a \approx 5.91 \times 10^{-3}$ and $b \approx 7.10 \times 10^{-3}$ come from the material properties of silicon. Notably, the four-fold symmetry of the crystal structure can be observed from the term $\cos 4\alpha$.

Additionally, if the spring beams are equally spaced apart, the resonance frequency is also affected by whether or not the number of spring beams matches the symmetry of the crystal lattice. For 3 beams, for example, the maximum predicted orientation effect is less than 1%, because each of the three beams is always at a different offset relative to the crystal lattice. Thus, the Young's moduli of the three beams are always averaged out, reducing the orientation dependence.

V. CONCLUSION

We explored how design factors such as the orientation of silicon and the number of suspension beams affect the characteristics of MEMS spring. Our results prove that the orientation of silicon in the device does affect the frequency the spring resonates at, and the number of suspension beams also affects the resonance. The effect is mostly consistent with a theoretical model involving the Young's modulus of the suspension beams. With the strict tolerances that MEMS spring can be designed with, these results suggest that both orientation as well as the number of beams are critical design parameters that must be considered in the fabrication of silicon MEMS devices.

ACKNOWLEDGMENT

The authors would like to thank Professor Kurt Broderick of MIT for his technical insights and lab supervision. The authors would also like to thank Professors Jesus A del Alamo and Jeurgen Schoenstein of MIT for their feedback and guidance throughout this exploration.

REFERENCES

- [1] M. Tilli, *Handbook of silicon based MEMS materials and technologies*. Elsevier, 2020.
- [2] P. Janin, D. Uttamchandani, and R. Bauer, "On-chip frequency tuning of fast resonant mems scanner," *Journal of Microelectromechanical Systems*, vol. 31, no. 6, pp. 977–983, 2022.
- [3] B. Khazaeili and R. Abdolvand, "Orientation-dependent acceleration sensitivity of silicon-based mems resonators," in *2016 IEEE International Frequency Control Symposium (IFCS)*, 2016, pp. 1–5.
- [4] D. M. Tanner, A. C. O. Jr., and F. Rodriguez, "Resonant frequency method for monitoring MEMS fabrication," in *Reliability, Testing, and Characterization of MEMS/MOEMS II*, R. Ramesham and D. M. Tanner, Eds., vol. 4980, International Society for Optics and Photonics. SPIE, 2003, pp. 220 – 228. [Online]. Available: <https://doi.org/10.1117/12.478201>
- [5] R. Dean, "Springs: Cantilever beams and mass-spring systems," Auburn University, Department of Engineering, Auburn, AL, Lecture Notes, 8 2022, covers cantilever beam springs, spring constants, fabrication issues, mass-spring system dynamics, and electrical-mechanical system equivalence. [Online]. Available: https://www.eng.auburn.edu/~dearon/Lecture_82422.pdf
- [6] M. A. Hopcroft, W. D. Nix, and T. W. Kenny, "What is the young's modulus of silicon?" *Journal of Microelectromechanical Systems*, vol. 19, no. 2, pp. 229–238, 2010. [Online]. Available: http://www.silicon.mhopeng.ml1.net.user.fm/Silicon/Hopcroft_Youngs_Modulus_Silicon.pdf